Bacteria metabolic adaptation to oxidative stress: the case of silica

Mercedes Perullini, Sophie Dulhoste, François Ribot, Gérard Pehau-Arnaudet, Odile Bouvet, Jacques Livage, Nadine Nassif

PII: S0168-1656(23)00140-2

DOI: https://doi.org/10.1016/j.jbiotec.2023.08.002

Reference: BIOTEC9262

To appear in: *Journal of Biotechnology*

Received date: 18 May 2023
Revised date: 25 July 2023
Accepted date: 7 August 2023

Please cite this article as: Mercedes Perullini, Sophie Dulhoste, François Ribot, Gérard Pehau-Arnaudet, Odile Bouvet, Jacques Livage and Nadine Nassif, Bacteria metabolic adaptation to oxidative stress: the case of silica, *Journal of Biotechnology,* (2023) doi:https://doi.org/10.1016/j.jbiotec.2023.08.002

Bacteria metabolic adaptation to oxidative stress: the case of silica

Mercedes Perullini,[1] Sophie Dulhoste[1], François Ribot[2], Gérard Pehau-Arnaudet[3], Odile Bouvet[4], Jacques Livage *[2] and Nadine Nassif[2]*

[1] CONICET - Universidad de Buenos Aires. Instituto de Química Física de los Materiales, Medio Ambiente y Energía (INQUIMAE). Laboratorio de materiales funcionales con actividad biológica. Buenos Aires, Argentina.

[2] Sorbonne Université, CNRS, Laboratoire de Chimie de la Matière Condensée de Paris (LCMCP), F-75252, Paris Cedex 05, France

[3] Institut Pasteur/ Ultrastructural BioImaging Core and UMR 3528, 75015 Paris, France.

[4] IAME, UMR 1137, INSERM, Univ Paris Diderot, Sorbonne Paris Cité, F-75018, Paris, France.

* Corresponding authors : mercedesp@qi.fcen.uba.ar; jacques.livage@sorbonne-universite.fr

Abstract

Although the presence of silica in many living organisms offers advanced properties including cell protection, the different *in vitro* attempts to build living materials in pure silica never favoured the cells viability. Thus, little attention has been paid to host-guest interactions to modify the expected biologic response. Here we report the physiological changes undergone by *Escherichia coli* K-12 in silica from colloidal solution to gel confinement. We show that the physiological alterations in growing cultures are not triggered by the initial oxidative Reactive Oxygen Species (ROS) response. Silica promotes the induction of alternative metabolic pathways along with an increase of growth suggesting the existence of *rpoS* polymorphisms. Since the functionality of hybrid materials depends on the specific biologic responses of their guests, such cell physiological adaptation opens perspectives in the design of bioactive devices attracting for a large field of sciences.

Keywords: Silica nanoparticles; living materials; physiological adaptation; oxidative stress; *rpoS* polymorphisms; confinement

1. INTRODUCTION

Silica is considered to be chemically and mechanically inert, thermally stable and resistant to microbial attack [1]. It is found in many living organisms including diatoms, bacteria and plants, as well as in higher animals, and it is also widely used for the production of goods or as additive in the food industry [2,3]. It also behaves unexpectedly as a glue for a large variety of applications [4] including clinical, surgery, and regenerative medicine [5]. Cellular encapsulation in silica has gained importance in the field of material science, allowing the development of host-guest multifunctional materials (HGMFs) with novel and varied applications, from medicine to catalysis [6,7]. In the recent years, efforts in the field of HGMFs development have been mainly focused on the diversification of encapsulated cell types. As a result, the range of potential biotechnological applications of these "living materials" has enormously increased [8]. A singular approach was to keep alive isolated cells in an inorganic silica matrix [9] and further study cell-to-cell communication through *quorum sensing* molecules [10,11]. In contrast, many procedures were developed for cellular division and growth inside silica matrices. Among them, a pre-encapsulation of the biological guest in a Ca(II)-alginate matrix [12] that confers protection from cytotoxic precursors during the synthesis of the silica network, resulting in improved cellular viability and preserved biological activity. This synthesis strategy is of high interest since typical responses of living cells in nature could, in principle, be reproduced in a near-natural environment provided by an internal liquid cavity within the silica matrix [13]. Therefore, creating space inside these matrices allowed the development of new applications that required a large number of metabolically active cells to render them efficient, or the growth of tissues or even whole organisms, such as small metazoans, inside an encapsulation matrix [14,15]. Moreover, hierarchically-engineered mesoporous silica nanoparticles lead to the generation of highly complex and nature-mimicking structures,[16,17] with applications in different fields of biomedicine, including drug delivery, bioimaging, and tissue engineering [18,19].

Perhaps the most important question to address is up to what extent a silica matrix is innocuous to the life developing inside. Though living organisms have been exposed to nanosized particles (NPs) throughout their evolutionary stages, such exposure has increased dramatically over the last century due to anthropogenic sources [20]. The particularities of engineered materials such as

microstructure and texture, shape, surface area, surface charge, chemical composition, surface functionalization[21], among others, may significantly differ from natural occurring nanoparticles or nanostructured materials, having a huge impact on the cellular uptake and toxicity.[22,23] Silica, as any other environmental stimulus, could modify the expected biological response [24–26]. Thus, managing this silica-cellular interplay constitutes an important challenge for scientists in different fields including inorganic chemistry, cellular biology, material science, biotechnology but also medicine as mentioned above. This prompted us to further investigate the effect of silica on the cellular growth and physiological states of bacteria.

For this purpose, *Escherichia coli* K-12 was used as a model bacterium to evaluate the physiological changes produced by contact with colloidal silica nanoparticles, as well as by encapsulation in a typical silica matrix obtained by the sol gel procedure. Many of the HGMFs are designed to generate self-supporting devices in which a certain biological function form of the encapsulated microorganism is required. Cellular stress during the synthesis of the encapsulation matrix (due to bioavailable precursors) has proved to be a major concern when it comes to not altering the biological response. [25] Commercial silica colloidal particles such as Ludox HS-40® are usually used in the sol gel synthesis following the aqueous route in replacement of part of the silica precursors to reduce the osmotic stress generated by soluble silicates. Small dense silica nanoparticles may be present in the medium, both as synthesis precursors not yet consumed and as particles detached by erosion of the initially consolidated encapsulation matrix or hierarchical mesoporous nanoparticle. Thus, since the presence of silica may be also considered as an environmental stress, the production of Reactive Oxygen Species (ROS) causing progressive oxidative damage and ultimately cell death needs to be evaluated. Indeed, ROS include the superoxide anion (O_2^-), hydrogen peroxide (H_2O_2) and hydroxyl radicals ($OH\cdot$); all of which are generated accidentally as by-products of aerobic metabolism and have inherent chemical properties that confer reactivity to different biological targets. This explains why they are often associated with oxidative stress, and the induction of pathology by damaging lipids, proteins and DNA. However, nowadays it is well accepted that one specific ROS, namely H_2O_2, is produced by mitochondria as signalling molecule in the maintenance of physiological functions [27].

Here, we show that silica induces an imbalance in the redox state and a clear alteration in cellular growth of *E. coli* K-12 producing a switch from fermentative to aerobic metabolism and even changing the nutritional capability of this strain. Interestingly, both physical silica systems (solution or gel) had a significant impact on the metabolic abilities of *E. coli*, producing faster cellular growth and an associated alteration in nutrition capabilities. The same alterations were observed in a mutant lacking *rpoS* (ΔrpoS). To our knowledge, cytotoxicity of inorganic nanoparticles is always reported in the literature while no study has ever shown a benefit in using them for cellular adaption. We also show that the redox response is mediated by a specific augmentation of intracellular H_2O_2 by analyzing the implications on cellular viability after silica encapsulation of *E. coli* mutants lacking different regulators of the redox response (Δ*oxyR*, Δ*soxR* and Δ*fur*) and by assessing the activity of hydroperoxidase I (HPI) and II (HPII), antioxidant enzymes that degrade H_2O_2 into water and oxygen.

To further understand silica-cell interactions, we analyzed the changes of glucose catabolism due to the presence of colloidal silica in the culture medium and evaluated the changes in nutritional capability of *E. coli* K-12 in the presence of colloidal silica or encapsulated within a silica hydrogel. Taken as a whole, these observations ruled out the initial hypothesis of the elevated ROS being a bare consequence of augmented cellular growth. A last arising question was if the observed physiological changes, including the induction of alternative metabolic pathways along with a clear alteration of the growth cycle, were induced by the initial increase in H_2O_2 concentration. We demonstrated that ROS scavengers, which avoid the increase in H_2O_2 do not prevent the physiological changes induced by silica. This suggests that they are independent of the moderate redox response. On the other hand, we found out that the observed phenotype corresponds to a mutant in the *rpoS* gene, which encodes for an alternative sigma factor in *E. coli*, responsible for the expression of ~10 % of genes and having a major impact not only on stress tolerance but also on the entire cell physiology under suboptimal growth conditions. Finally, these results provide new insights on the role of the mechanical (gel condensation) *vs*. chemical (particles in solution) effects on cell behaviour, which are fundamental to set new efficient hybrid living materials.

2. MATERIALS AND METHODS

Microorganisms culture conditions. Five strains of *E. coli* were employed in these experiments: three single gene deletion mutants implicated in the redox response (Δ*oxyR*, Δ*soxR* and Δ*fur*), a knockout for *rpoS* gene implicated in the onset of stationary phase (Δ*rpoS*) from Keio collection n°MG1655 and wild-type host strain (BW 25113) [28,29]. All strains were pre-cultured in Luria Bertani (LB) broth, a nutritionally rich medium, at 37 °C and stirred on a rotary shaker to maintain sufficient culture aeration (180 rpm). Cells from the overnight culture in LB at 37°C were centrifuged and washed three times with a minimal medium (MM) without carbon source (100 mM NaCl, 30 mM triethanolamine HCl, 5 mM NH_4Cl, 2 mM NaH_2PO_4, 0.25 mM Na_2SO_4, 0.05 mM $MgCl_2$, 1 mM KCl, 1 mM $FeCl_3$, pH 7.1) and finally dissolved in the same MM.

For growth assessment, MM supplemented with 10 mM glucose (MMG) was added to the overnight culture of the wild type strain to obtain 10^6 bacteria/ml. When indicated, aliquots of this inoculated broth were mixed with SiO_2 commercial nanoparticles (Ludox HS-40 ®, from Sigma Aldrich; diameter: 12 nm) or with hydrogen peroxide (30% (w/w) in H_2O; Sigma Aldrich). Different volumes of the inoculated broth were poured on 50 mL vessels and grown at 37°C and stirred on a rotary shaker at 120 rpm. Anaerobic conditions were fixed by the ratio of liquid culture volume to total flask volume. Each experiment was performed in triplicate. From each growth curve (optical density at 600 nm (OD_{600}) *vs.* culturing time), instant growth rates were calculated by deriving a smoothing spline fitted to the logarithm of the OD_{600}. The rate of exponential growth is expressed as generation time, G, where G = ln2/growth rate. The lag time was measured as the time to reach the onset of exponential phase.

For cellular encapsulation experiments, aliquots of MM supplemented with 10 mM glucose (MMG) were added to the overnight cultures to obtain 10^6 bacteria/ml of each of four strains (Δ*oxyR*, Δ*soxR*, Δ*fur* and *wt*). These cultures were grown at 37 °C, stirred on a rotary shaker (180 rpm) and harvested in early exponential phase.

Silica encapsulations. This procedure was performed as previously described [26]. An aliquot (2 ml) of a culture of exponentially growing cells (OD_{600}: 0.6–0.8) was collected by centrifugation, washed three times and finally re-suspended in 2 ml of physiological solution (stock cellular suspension). Aliquots of 100 µl of these suspensions were encapsulated at room temperature by mixing volumes of the different precursor solutions to obtain a SiO_2:water molar relation of 3.8 with a fixed proportion of polymeric to particulate silica precursors (1:4) at constant pH = 7.0, adjusted with HCl and immediately vortexed for 30 sec.

For viability assays, at the specified times *(i.e.* 1 and 7 days), samples were disrupted mechanically and dissolved in physiological solution. Viability was assessed by traditional plate counting in LB-agar, informing the viability as % with respect to the initially encapsulated cell number, given by the number of CFU obtained for the stock cellular suspension (taking into account the dilution in samples). Six replicates were prepared of each encapsulation sample.

Intracellular Reactive Oxygen Species (ROS). To assess the level of intracellular ROS, an aliquot (2 ml) of a culture of exponentially growing cells (OD_{600}: 0.6–0.8) was collected by centrifugation, washed three times, re-suspended in 2 ml of physiological solution (stock cellular suspension) with a fluorescent probe (2'-7'-dichlorofluoresceine diacetate, Sigma Aldrich) and incubated at 30°C in the dark for 30 min. The level of intracellular ROS of bacteria submitted to different treatments (contact with silica nanoparticles with increasing silica concentration or encapsulation) was quantified using a microplate reader (FLUOstar OPTIMA®) in fluorescence intensity mode.

***Catalase activity*.** This procedure was performed as previously described [30]. The reagents used are hydrogen peroxide solution (30% (w/w) in H_2O_2; Sigma Aldrich), 1% Triton X-100 (Sigma Aldrich), and catalase from bovine liver (3000 units/mg solid; Sigma Aldrich). Catalase powder was dissolved in 100 µl of distilled water to prepare each concentration of catalase standard. To quantify the catalase activity, a calibration curve was plotted with the defined unit of catalase activity. Each catalase solution (100 µl) or bacterial suspension (100 µl) was added in a Pyrex tube (13 mm diameter-100 mm height, borosilicate glass). Immediately, 100 µl of hydrogen peroxide solution and 100 µl of 1% Triton X-100 were added and the solutions were mixed vigorously then incubated at room temperature (20 ^{0}C). Following completion of the reaction, the height of O_2-forming foam was finally measured using digital images analysed using imageJ (version 1.49) free software. In order to distinguish between the activities of heat-labile catalase HPI and heat-stable catalase HPII, the aliquot of 100 µl of bacterial suspension was exposed to heat treatment (55 ^{0}C; 15 min) and the residual catalase activity following heat treatment was subtracted from the total catalase activity to determine the activity of the heat-labile catalase.

CryoTEM. As described for the encapsulation in silica, bacteria suspensions were prepared from culture stopped at the exponential stage (OD_{600}: 0.6–0.8). Observations were performed on a Jeol 2010F operating at 200 kV under low dose conditions (15 electrons/Å^2.second) using a Gatan (USA) ultrascan 4000 camera. One drop of bacteria suspensions was mixed with colloidal SiO_2 (*i.e*. 0.01, 0.1 or 1 wt%) or without (control) with glucose. Then, the four resulting different bacteria suspensions were deposited on a R2/2 Quantifoil grid (Germany). The grid was cryofixed in liquid ethane using a cryo-fixation device (EMGP, Leica, Austria). Samples were transferred inside the microscope with a Gatan 626DH cryoholder (USA).

***^{13}C-NMR*.** Culture conditions were performed as described above except for the MMG broth, which was supplemented with [1-^{13}C] glucose. At different culture times, 500 µl of the samples were introduced into a 5 mm NMR tube. A coaxial insert containing D_2O with 10% TMSP (3-trimethylsilyl propionic-2,2,3,3-δ4 acid sodium salt) was added as a chemical shift reference ($\delta(^{13}C)_{TMSP}$ = -2.0 ppm.) and for locking purpose. All ^{13}C NMR spectra were recorded under the same conditions (30° flip angle, ^{1}H power gated decoupling, 3s recycling delay, 256 transients) at 20°C on a Bruker Av^{III} 300 spectrometer (75.47 MHz for ^{13}C) equipped with a BBFO probe. Therefore, the absolute intensity of NMR peaks is significant of the amount of each species in the sample.

Statistical Analysis. Data were analyzed using one-way analysis of variance (ANOVA) with Tukey's post-test using Prism 6.01 (GraphPad Software Inc., San Diego, CA, USA). When the ANOVA indicates differences between means, a t-test was used to differentiate the means with 95% confidence ($p < 0.05$). Principal component analysis (PCA) was performed using the 'R' software (http://www.R-project.org). PCA facilitates the simultaneous comparison of a large number of complex objects, such as the degree of utilization of 96 different carbon sources (observations) and the treatments to which bacteria were exposed (variables), such as liquid culture with or without the addition of different concentrations of silica nanoparticles or the encapsulation in a silica matrix. From the PCA analysis, it was determined that two main components, F1 and F2, explained the 93.1 % of the total variation in C-source utilization patterns, and can be used to statistically summarize the signature of intersample variations.

Silica increases growth-rate and biomass yield. Strikingly, in our first attempt of creating a near-natural environment for cell division and growth within a silica monolith almost two decades ago, we found that the growth rate of the microorganisms inside the host matrix presented no significant differences with control samples in conventional liquid culture media [13]. Assuming silica impact on living cells to be negligible, these results are still surprising since a lower growth rate was expected due to a delayed diffusion of nutrients and metabolic waste products [31]. Furthermore, poorer availability of oxygen inside the material's cavities compared to aerated liquid culture conditions should result not only in a lower growth rate but also in a lower cellular density at the stationary phase. Thus, a possible explanation for this unexpected result is that the effect of silica was counteracting the drop in bacterial growth caused by confinement in small voids with lower aeration and delayed transport of metabolites. To test this hypothesis, we evaluated the effect of adding silica nanoparticles to liquid cultures of *E. coli* K-12 (minimal medium with glucose, MMG) submitted to low aeration conditions (similar to what is expected for cellular encapsulation devices). As shown in **Figure 1-A**, with the addition of commercial silica nanoparticles (SiO_2 NPs), in a final concentration of 0.4 % SiO_2 in weight to the culture medium, although the lag phase of growth became longer (1.5 h *vs*. 0.5 h), the growing rate increased during the exponential phase with a generation time, G, of 0.84±0.04 h instead of 1.06±0.05 h for the control culture (*i. e.*, without the addition of SiO_2 NPs). Furthermore, the entrance in the stationary phase was significantly retarded, reaching a higher cell density at late stationary phase (a 3-fold growth is observed for the optical density at 600 nm (OD_{600}), after 24 h of culture: 1.60±0.15 for the culture added with SiO_2 NPs vs. 0.51±0.06 for the control). Because aggregation of nanoparticles may occur with scattering in the visible region and artifact in OD_{600} data, traditional plate counting technique was also performed confirming the 3-fold increase in biomass yield, evaluated from colony forming units (CFU) counting (control = 1.4±0.2 x 10^8 CFU/mL; culture added with SiO_2 NPs = 4.4±0.5 x 10^8 CFU/mL).

To go further on the understanding of such effect, we analyzed the ^{13}C-NMR spectra of *E. coli* K-12 after 7 hours of culture in minimal medium supplemented with D-glucose-1-^{13}C with or without

the addition of SiO_2 NPs. As shown in **Figure 1-B**, while glucose is almost depleted in the culture added with SiO_2 NPs (8.3 % of initial supply of glucose remaining), the control sample retained a 24.4% of the initial concentration of glucose. It is worth noting that 7 hours of culture corresponds to the entrance to the stationary phase for the control sample, meanwhile this transition occurs 1.5-2 hours later for the sample treated with silica. It is described that many microorganisms switch from a physiological program that permits rapid growth in the presence of abundant nutrients to a life-style that enhances survival in the absence of those nutrients. One such change in nutritional capability occurs when bacterial cells transit from a program of rapid growth that produces and excretes acetate to a regime of slower growth based on their ability to scavenge for environmental acetate. This acetate-switch is described to occur as cells deplete their environment of acetate-producing carbon sources, such as glucose [32]. However, in the presence of SiO_2 NPs, the sustained growth in spite of the meagre supply of glucose during the late exponential phase indicates the simultaneous utilization of another substrate as a carbon source. This is confirmed by the ratios acetate/lactate and acetate/succinate, which are significantly reduced with respect to the control sample: 4.3 (control) *vs.* 1.7 (SiO_2 NPs), and 6.3 (control) *vs.* 5.4 (SiO_2 NPs), respectively. The increase in cellular density seems to be concomitant with the consumption of acetate from the medium, Therefore, silica might be deregulating the diauxic scheme (in which the metabolism of nutrients is strictly sequential) to promote the consumption of acetate in the presence of glucose in the culture medium.

As shown in **Figure 1-CI**, the addition of SiO_2 NPs leaded to an increase of the biomass yield in a dose-dependent manner. Even at a very low concentration (0.02 % of SiO_2 in weight) a statistically significant difference in the OD_{600} in late stationary phase is evidenced. Cellular growth reached the asymptotic value of $OD_{600} \approx 2.2$ (i. e. 50% higher than for the control sample) for a 0.3 % of SiO_2 in the culture medium. Thus, this concentration, maximizing effect/dose relation, was selected for the following experiment aimed to assess the effect of silica under different aeration conditions (**Figure 1-CII**). The aeration of cultures was modulated as previously reported by changing the ratio of liquid culture volume to total flask volume [33,34]. As expected, both series of samples followed the same trend: biomass yield is increasing with the aeration of culture (given by lower

culture volume fraction). *E. coli* is a metabolically versatile bacterium that experiences transitions between aerobic (outside a host) and anaerobic (in the lower intestine of a host) niches as part of its lifestyle. Therefore, the ability to adapt to environments with different O_2 availabilities is vital for its competitiveness in nature. When O_2 is available, aerobic respiration allows the complete oxidation of glucose with much higher energy yield than anaerobic respiration or fermentation. However, regardless of the aeration condition, a significantly higher biomass is obtained for SiO_2 treated samples. The pH value of culture media at stationary phase is an indirect measure of cellular metabolism: at lower aeration conditions, the acidification of culture can be explained by a higher accumulation of acidic overflow metabolites, such as acetate, lactate and succinate. On the other hand, in the presence of SiO_2 NPs, the culture media acidification effect caused by poorer O_2 availability is compensated with the consumption of acetate as a carbon source, giving higher pH values after 24 hours of culture (**Figure 1-CIII**). It is worth noting that an effect of the basification due to Ludox-HS40 solution is discarded, since the culture media was neutralized immediately after its addition on the treated samples.

In the next step, we investigated if the oxidative imbalance is a cause or a consequence of this change in the metabolic pathways.

On the trail of silica's mode of action – ROS: the usual suspects. One of the main mechanisms in the cytotoxic action of nanosized particles involves the development of oxidative stress, which consists in high intracellular levels ROS, by-products of aerobic metabolism that cause damage to lipids, proteins and DNA [35,36]. ROS include the superoxide anion (O_2^-), hydrogen peroxide (H_2O_2), and hydroxyl radicals (OH•), which differ from O_2 in having one, two, and three additional electrons, respectively. ROS are present at low, non-toxic concentrations during normal metabolism. When the level of ROS increases, many enzymes protect against oxidative damage in *E. coli* [37]. However, and far from being detrimental, a slight increase in ROS regulates cell signalling pathways that allow their adaptation to changes in the environment [38]. H_2O_2 is implicated as the main transmitter of redox signals; *E. coli* submitted to a low-grade H_2O_2 stress responds by

activating both the OxyR defensive regulon and the Fur iron-starvation response. On the other hand, an increase in O_2^- concentration activates the genetic locus SoxR [39].

In order to evaluate if the contact with SiO_2 NPs and/or the encapsulation in silica matrices elicits an oxidative imbalance, the formation of intracellular ROS was quantified using the fluorescent probe, 2',7' dichlorofluorescein-diacetate (DCFH-DA). DCFH-DA enters the cells and is oxidized by ROS to fluorescent dichlorofluorescein (DCF). The DCF generated is directly proportional to intracellular concentration of ROS, as previously reported [40]. As positive control, H_2O_2 was added at different concentrations to control samples (*i.e.* bacteria in liquid culture medium without SiO_2 NPs) to generate an oxidative perturbation, see **Figure 2-AII**. A linear response in the fluorescence intensity, indicative of the level of intracellular ROS, was observed for all the strains as a function of H_2O_2 concentration (up to 500 µM). It is worth noting that mutants lacking different genes implicated in the redox regulation (Δ*oxyR* and Δ*soxR*) showed a similar response slope with respect to the *wt* strain, although presenting higher basal levels of intracellular ROS. As shown in **Figure 2-AI**, very low concentrations of SiO_2 NPs elicited a noticeable increase in intracellular ROS level. For example, 0.01% SiO_2 produced an intracellular ROS level in the *wt* strain comparable to that caused by 300 µM H_2O_2. SiO_2 NPs generated a dose-dependent response, analogous to the effect observed for the addition of H_2O_2, showing a slight decrease in ROS levels for the higher concentrations assayed (> 0.3% SiO_2). As expected, for mutants in the oxidative response, the basal level of intracellular ROS was higher than in the *wt* strain and the oxidative response triggered by silica followed the same dose-dependent trend, translated upwards in the ordinate axis. Also in line with strains lacking mechanisms of response to oxidative damage, no regulation of ROS levels was observed in the mutant strains for high concentrations of SiO_2 NPs. The level of intracellular ROS recorded 30 minutes after matrix gelation in the case of encapsulation in silica (with a total SiO_2 concentration of 10 % in weight), was similar to that observed for SiO_2 NPs in the range of 0.1 – 1.0 %. This result is not surprising, as when gelation occurs, SiO_2 NPs aggregate forming clusters and structures of higher hierarchy, being less bioavailable and generating lower cytotoxic effects than a suspension of NPs at a concentration of 10% of SiO_2.

To evaluate long-term effects, the viability of *wt E. coli* and mutants of oxidative response genes was assessed as a function of the time elapsed encapsulated inside a silica hydrogel (initial viability, after 1 day of encapsulation and after 7 days of encapsulation). As shown in **Figure 2-B**, the viability of Δ*oxyR* mutant was undetectable (<0.1%), even 30 minutes after silica matrix gelation *(i.e.* initial viability). It has been demonstrated that H_2O_2 can function as a signalling molecule owing to its ability to induce fully reversible protein modifications, inducing glutathionylation of cysteine residues or sulphoxidation of methionine residues in various targets [41]. These targets include the transcription factor OxyR in bacteria, which in turn induces the transcription of genes necessary for the bacterial defence against oxidative stress [42], thus providing a mechanism of self-regulation. The extreme sensibility of Δ*oxyR* mutant towards silica encapsulation indicates the increase in intracellular levels of H_2O_2. On the other hand, viability of Δ*soxR* mutant that reflects the regulation of the oxidative stress response dependent on superoxide [43], does not show any significant difference with the *wt* after 1 day. The loss of viability observed for the Δ*fur* mutant (regulator of intracellular iron) further supports the hypothesis of an increase production of H_2O_2, as it has been shown that peroxide stress elicits adaptive changes in bacterial metal homeostasis [44]. Therefore, the presence of colloidal silica in the culture medium selectively increases the intracellular level of H_2O_2.

To go further, an important question was whether this oxidative imbalance is a consequence of an increased rate of cellular division (*i.e.* an augmented aerobic metabolism activity) or on the contrary, the elevated intracellular ROS concentration is involved in the activation of signalling pathways to promote proliferation and metabolic adaptation.

Relation between the redox signalling pathways and the cellular growth in silica. It is well established that endogenous oxidative stress produces diversity and adaptability in bacteria [45]. To determine whether the effect observed with silica is triggered or not by redox-signalling pathways, the catalase activity was measured during the growth curve. In general terms, a high rate of reactive oxygen species (ROS) production is counterbalanced by an equally high rate of antioxidant activity in order to maintain redox balance [46]. Catalase is a ubiquitous antioxidant enzyme that degrades

H_2O_2 into water and oxygen. There are two catalase enzymes in *E. coli*, hydroperoxidase I (HPI) and II (HPII), which are induced independently. While HPI is transcriptionally induced during logarithmic growth in response to low concentrations of H_2O_2 in a OxyR dependent manner, HPII is *(i)* positively regulated by RpoS (RNA polymerase, sigma S, implicated in the onset of stationary phase), *(ii)* is not peroxide inducible and *(iii)* is a key player in survival during the entrance in stationary phase and other stresses [47]. Consequently, to correlate the perturbation observed in redox balance with the differences in the cellular growth behaviour, we measured both catalase activities at different phases of cellular growth of a wild type strain (*wt*) and a mutant lacking the *rpoS* gene (Δ*rpoS*). Similar experiments carried out with a mutant lacking the *oxyR* gene (Δ*oxyR*) were not conducted since the viability of this strain is affected by the presence of SiO_2 NPs. As shown in **Table 1**, in the presence of SiO_2 NPs, HPI activity increased during the early exponential phase (EEP) both in *wt* and Δ*rpoS* strains. This may be due to the documented increase in intracellular concentration of H_2O_2 found in samples in contact with SiO_2 NPs as discussed above. During late exponential phase (LEP), the rate of cellular division of samples submitted to SiO_2 NPs was found to be much higher than in control samples while the HPI activity did not show any significant differences between control and silica treated samples. This indicates that the rise in intracellular H_2O_2 level is not a direct consequence of increased aerobic metabolism. Additionally, during the LEP, HPII activity in silica treated *wt* samples, far from being increased, is 3-fold diminished with respect to control. Thus, catalase activity of HPII is suggestively lower when SiO_2 NPs are added to *wt* bacteria, suggesting that the effect elicited by silica (*i.e.* delayed entrance in stationary phase) is not directly triggered by H_2O_2. Finally, further experiments ensure that adding H_2O_2 at different concentrations during the growth curves of *E. coli wt*, does not reproduce the effect caused by silica addition in the culture medium and, at the same time, the effect caused by silica on *E. coli* growth is not prevented by ROS scavengers (see supplementary information). Although these results showed no apparent relationship between the observed increase in intracellular ROS level and the deregulation in growth induced by silica, they offered an important hint: the activity of HPII is very low during the LEP for the silica treated *wt* sample. The fact that the *wt* strain in contact with SiO_2-NPs showed similar activity of HPII than Δ*rpoS* mutants indicates that silica

possibly downregulates the RpoS regulon. The *rpoS* gene encodes the master regulator of stress σ^s. σ^s protein is the second most important sigma factor in *E. coli* and is responsible for the expression of ~10 % of genes, having major impact not only on stress tolerance but on the entire cell physiology under suboptimal growth conditions. Under nutrient deprivation or different stresses such as a subinhibitory concentration of antibiotics or the immobilization in biofilms or agar plates, signalling cascades leading to RpoS induction prepare cells for the entrance in stationary phase increasing their resistance [48–50]. On the contrary, the contact with silica showed the opposite effect: a decrease in HPII activity, a protein which expression is positively regulated by RpoS. Furthermore, a downregulation in RpoS could also explain the retarded entrance in stationary phase, the main anomaly in growth curves observed with silica treatment.

Changes in phenotypic and nutritional capability. Different levels of RpoS are a major source of phenotypic differences. Cryo-Transmission Electron Microscopy (cryo-TEM) observations were performed to investigate the possible changes in bacterial structures when silica is added into the medium. Using cryo-TEM ensures to avoid drying artefacts (*e.g.* the formation of artificially colloidal aggregates). Cultures of *E. coli* K-12 with SiO_2 NPs concentrations in the range 0.01 to 1 wt% were observed, comparing to a suspension of *E. coli* K-12 without added SiO_2 NPs as a control sample. Fimbriae are observed but they appear not to interact with the SiO_2 NPs (**Figure 3a**). Interestingly, this is also observed with bacteria freshly encapsulated in silica hydrogels while a strong interaction is found upon ageing [51]. For 1% of SiO_2 NPs, the distribution of the particles is more homogeneous with less aggregation (**Figure 3b**). Further observations show a gap between the particles and the bacterium's wall. This suggests low chemical interactions between cells and SiO_2 NPs (**Figure 3c**) although fimbriae are described to have adhesive properties. Interestingly, the presence of fimbriae appears to increase with the silica concentration (**Figure 3d**), which is in agreement with previous works showing that *(i)* the repression of fimbriae formation are no longer seen in strains deficient in RpoS [52] *(ii)* the fimbriation is related to the reduced state of OxyR [53]. All these results emphasize that the effect of silica on the bacterial growth is not due to mechanical processes but to physiological changes.

RpoS has also a pleiotropic role on metabolic capacity, metabolic abilities being inversely related to stress resistance. Thus, a strain with a high level of RpoS is resistant to oxidative stress (high level of hydroperoxidase II) and has low nutritional capacities. Conversely, a strain with low RpoS is sensitive to oxidative stress but can use a greater number of carbon sources. While *rpoS* is expected to be conserved due to its central role in adaptation to a changing environment, mutations occur and spread at rapid rates in glucose-limited culture conditions. These mutants reduce σ factor competition and improve nutrient scavenging by increasing the expression of genes involved in vegetative growth, induced by RpoD, the main sigma factor in *E. coli* [54].

As discussed above, in the presence of SiO_2 NPs, the accumulated acetate seems to be used by *E. coli* K-12 even before the complete depletion of glucose in the culture medium. This implicates that the sole presence of SiO_2 in the form of NPs is affecting the nutritional capabilities of *E. coli*, which in turn could be related to the induction of mutations with loss of function in *rpoS*. In order to corroborate this hypothesis, we analysed the effect of SiO_2 (both as NPs in the culture medium and as encapsulation hydrogel matrix) on the nutritional profile of this microorganism (*wt* or *ΔrpoS* mutant) by testing the utilization of different carbon sources with the commercial Biolog® microplate system (96 substrates).

Principal component analysis (PCA) was performed on a subset of carbon sources (C-sources) where changes in the degree of use were evidenced in at least one treatment. Two main components explaining the 93.1 % of the total variation, F1 (57.7 %) and F2 (35.4 %), were selected, and both the variables (different treatments) and the observations (C-sources) were projected on the two axes of the PCA (**Figure 4**). The corresponding data are available in Supplementary Information (Table S2). The first PCA axis explains the 57.7 % of the total variation and differentiates encapsulated bacteria *versus* those bacteria in culture with or without the addition of SiO_2 NPs. The second PCA axis explains the 35.4 % of the total variation and separates the substrates with an increased consumption from those with a reduced utilization in the presence of silica. From these data, it can be concluded that the contact with silica elicits important changes in the nutritional profile of *E. coli* K-12. It is worth noting that for the 10 substrates for which the presence of silica (both as encapsulation matrix or added as NPs in suspension in the culture medium)

increases their utilization, the *ΔrpoS* mutant also showed an increased consumption. On the other hand, for 9 C-sources a decrease or even null utilization by encapsulated cells was evidenced (both, *wt* and *ΔrpoS*), which could be partly attributed to a limited transport through the silica hydrogel [31]. Nevertheless, the changes elicited by silica encapsulation in the nutritional profile correlated with those detected for a *rpoS* mutant (the correlation factor from PCA analysis is significantly different from 0 at the P=0.05 level). Mutations in rpoS are the most common growth advantage in stationary-phase (GASP) mutations found in aged *E. coli* cultures, and it has been reported that they increase the ability to use alanine, aspartate, glutamate, glutamine, serine, threonine and proline as sole sources of carbon and energy [55], which coincide with our observation of the main metabolic changes trigged by silica. Remarkably, this advantageous phenotype reported to occur in long-term starvation conditions -typically after 10 days- [56] was observed within a few hours and before glucose depletion in silica encapsulation systems.

Given that, as a whole, the alterations in *E. coli* K12 produced by silica that we have observed throughout this work are varied. The main results are schematically shown in **Figure 5** and all the results are sum up in **Figure 3S**, in supplementary information.

4. CONCLUSIONS

The combination of living cells with sol-gel silica is a promising strategy for the design of a myriad of advanced applications. However, a deep understanding of silica-cellular interactions is imperative. Here we demonstrate that, far from being inert, silica leads to complex changes at a metabolic level in *E. coli* K 12. Physiological alterations induced by silica cannot be derived from previously observed imbalance in the oxidative status of the cell. They include broadened nutritional profile, increase in growth-rate and biomass yield and augmented sensitivity to H_2O_2 in the late exponential phase. Along with the catalase activity of Hydroperoxidase II, metabolic analysis suggests a deregulation of RNA polymerase, σRNfactor (rpoS), which may also explain the observed delayed entrance in the stationary phase. The presence of fimbrae at high level of silica strengthens a low rate of Rpos and the reduced form of OxyR, which are of high interest for

antimicrobial applications in limiting bacterial aggregation, microcolony and biofilm formation. Further studies beyond the scope of this paper will help to confirm the regulation on RpoS and to elucidate the mechanism of the increased mutation rate, as well as to perform the analysis of individual mutants. We found qualitative differences between the changes induced by SiO_2 nanoparticles in solution and those generated by the encapsulation in a silica hydrogel matrix, suggesting that measurements at the population level could be biased by a substantial heterogeneity. Such important changes in cellular physiology have significant implications for our understanding of bacterial signal transduction in different environments (*e.g*. human body) as well as in recent well-spread applications such as cellular encapsulations to create host-guest multifunctional materials or mesoporous nanoparticles for controlled delivery of bioactive molecules to target cells shedding light on the complex interactions between new anthropogenic materials and living cells.

ACKNOWLEDGEMENTS. This work was supported by the EULASUR Project 233467 (Network in advanced materials and nanomaterials of industrial interest between Europe and Latin American countries of MERCOSUR: Argentina-Brazil-Uruguay). MP thanks María Eugenia Monge and Gastón Paris for fruitful discussions.

BIBLIOGRAPHY

1. Meunier, C. F., Dandoy, P. & Su, B. L. Encapsulation of cells within silica matrixes: Towards a new advance in the conception of living hybrid materials. *J. Colloid Interface Sci.* **342**, 211–224 (2010).
2. Van Dyck, K., Van Cauwenbergh, R., Robberecht, H. & Deelstra, H. Bioavailability of silicon from food and food supplements. *Fresenius. J. Anal. Chem.* **363**, 541–544 (1999).
3. Bansal, V., Ahmad, A. & Sastry, M. Fungus-mediated biotransformation of amorphous silica in rice husk to nanocrystalline silica. *J. Am. Chem. Soc.* **128**, 14059–14066 (2006).
4. Rose, S. *et al.* Nanoparticle solutions as adhesives for gels and biological tissues. *Nature* **505**, 382–385 (2014).
5. Meddahi-Pellé, A. *et al.* Organ repair, hemostasis, and in vivo bonding of medical devices by aqueous solutions of nanoparticles. *Angew. Chemie - Int. Ed.* **53**, 6369–6373 (2014).
6. Nassif, N. & Livage, J. From diatoms to silica-based biohybrids. *Chem. Soc. Rev.* **40**, 849–859 (2011).
7. Tomczak, M. M., Stone, M. O. & Naik, R. R. Biomimetic silica encapsulation of nanoparticles and enzymes. *ACS Symp. Ser.* **986**, 171–182 (2008).
8. Harper, J. C. *et al.* Encapsulation of S. cerevisiae in poly(glycerol) silicate derived matrices: Effect of matrix additives and cell metabolic phase on long-term viability and rate of gene expression. *Chem. Mater.* **23**, 2555–2564 (2011).

9. Nassif, N. *et al.* Living bacteria in silica gels. *Nat. Mater.* **1**, 42–44 (2002).
10. Nassif, N., Roux, C., Coradin, T., Bouvet, O. M. M. & Livage, J. Bacteria quorum sensing in silica matrices. *J. Mater. Chem.* **14**, 2264 (2004).
11. Carnes, E. C. *et al.* Confinement-induced quorum sensing of individual Staphylococcus aureus bacteria. *Nat. Chem. Biol.* **6**, 41–45 (2010).
12. Posbeyikian, A. *et al.* Evaluation of calcium alginate bead formation kinetics: An integrated analysis through light microscopy, rheology and microstructural SAXS. *Carbohydr. Polym.* **269**, 1–10 (2021).
13. Perullini, M., Jobbágy, M., Soler-Illia, G. J. A. A. & Bilmes, S. A. Cell growth at cavities created inside silica monoliths synthesized by sol-gel. *Chem. Mater.* **17**, 3806–3808 (2005).
14. Perullini, M., Calcabrini, M., Jobbágy, M. & Bilmes, S. A. Alginate/porous silica matrices for the encapsulation of living organisms: tunable properties for biosensors, modular bioreactors, and bioremediation devices. *Mesoporous Biomater.* **2**, 3–12 (2015).
15. Perullini, M., Orias, F., Durrieu, C., Jobbágy, M. & Bilmes, S. A. Co-encapsulation of Daphnia magna and microalgae in silica matrices, a stepping stone toward a portable microcosm. *Biotechnol. Reports* **4**, 147–150 (2014).
16. Wong, Y. J. *et al.* Revisiting the Stöber method: Inhomogeneity in silica shells. *J. Am. Chem. Soc.* **133**, 11422–11425 (2011).
17. Song, H. *et al.* Silica Nanopollens Enhance Adhesion for Long-Term Bacterial Inhibition. *J. Am. Chem. Soc.* **138**, 6455–6462 (2016).
18. Kankala, R. K., Han, Y. H., Xia, H. Y., Wang, S. Bin & Chen, A. Z. Nanoarchitectured prototypes of mesoporous silica nanoparticles for innovative biomedical applications. *J. Nanobiotechnology* **20**, 1–67 (2022).
19. Vazquez Echegaray, C. *et al.* Design of silica nanocarriers: Tuning the release to embryonic stem cells by simple strategies. *J. Biotechnol.* **353**, 19–27 (2022).
20. Oberdörster, G., Oberdörster, E. & Oberdörster, J. Nanotoxicology: An emerging discipline evolving from studies of ultrafine particles. *Environ. Health Perspect.* **113**, 823–839 (2005).
21. Kankala, R. K. *et al.* Nanoarchitectured Structure and Surface Biofunctionality of Mesoporous Silica Nanoparticles. *Adv. Mater.* **32**, 1–27 (2020).
22. Häffner, S. M. *et al.* Membrane Interactions of Virus-like Mesoporous Silica Nanoparticles. *ACS Nano* **15**, 6787–6800 (2021).
23. Rancan, F. *et al.* Skin penetration and cellular uptake of amorphous silica nanoparticles with variable size, surface functionalization, and colloidal stability. *ACS Nano* **6**, 6829–6842 (2012).
24. Kuncova, G. *et al.* Monitoring of the viability of cells immobilized by sol-gel process. *J. Sol-Gel Sci. Technol.* **31**, 335–342 (2004).
25. Napierska, D., Thomassen, L. C., Lison, D., Martens, J. A. & Hoet, P. H. The nanosilica hazard: another variable entity. *Part. Fibre Toxicol.* **7**, 39 (2010).
26. Perullini, M., Jobbágy, M., Moretti, M. B., García, S. C. & Bilmes, S. A. Optimizing silica encapsulation of living cells: In situ evaluation of cellular stress. *Chem. Mater.* **20**, (2008).
27. Schieber, M. & Chandel, N. S. ROS function in redox signaling and oxidative stress. *Curr. Biol.* **24**, R453–R462 (2014).
28. Datsenko, K. A. & Wanner, B. L. One-step inactivation of chromosomal genes in Escherichia coli K-12 using PCR products. *Proc. Natl. Acad. Sci. U. S. A.* **97**, 6640–6645 (2000).
29. Baba, T. *et al.* Construction of Escherichia coli K-12 in-frame, single-gene knockout mutants: The Keio collection. *Mol. Syst. Biol.* **2**, (2006).
30. Iwase, T. *et al.* A simple assay for measuring catalase activity: A visual approach. *Sci. Rep.* **3**, 3–6 (2013).
31. Perullini, M., Jobbágy, M., Japas, M. L. & Bilmes, S. A. New method for the simultaneous determination of diffusion and adsorption of dyes in silica hydrogels. *J. Colloid Interface Sci.* **425**, (2014).

32. Wolfe, A. J. The Acetate Switch. *Microbiol. Mol. Biol. Rev.* **69**, 12–50 (2005).
33. McDaniel, L. E., Bailey, E. G. & Zimmerli, A. Effect of Oxygen Supply Rates on Growth of Escherichia Coli. *Appl. Microbiol.* **13**, 109–114 (1965).
34. Rahbani, J. *et al.* The effect of aeration conditions, characterized by the volumetric mass transfer coefficient KLa, on the fermentation kinetics of Bacillus thuringiensis kurstaki. *J. Biotechnol.* **210**, 100–106 (2015).
35. Imlay, J. A. The molecular mechanisms and physiological consequences of oxidative stress: lessons from a model bacterium. *Nat. Rev. Microbiol.* **11**, 443–454 (2013).
36. Guo, C. *et al.* Silica nanoparticles induce oxidative stress, inflammation, and endothelial dysfunction in vitro via activation of the MAPK/Nrf2 pathway and nuclear factor-κB signaling. *Int. J. Nanomedicine* **10**, 1463–1477 (2015).
37. Imlay, J. A. Cellular defenses against superoxide and hydrogen peroxide. *Annu. Rev. Biochem.* **77**, 755–776 (2008).
38. Winterbourn, C. C. & Hampton, M. B. Redox biology: Signaling via a peroxiredoxin sensor. *Nat. Chem. Biol.* **11**, 5–6 (2015).
39. Mancini, S. & Imlay, J. A. The induction of two biosynthetic enzymes helps Escherichia coli sustain heme synthesis and activate catalase during hydrogen peroxide stress. *Mol. Microbiol.* **96**, 744–763 (2015).
40. Rosenkranz, A. R. *et al.* A microplate assay for the detection of oxidative products using 2′,7′-dichlorofluorescin-diacetate. *J. Immunol. Methods* **156**, 39–45 (1992).
41. Choi, H. *et al.* Structural Basis of the Redox Switch in the OxyR Transcription Factor. **105**, 103–113 (2001).
42. Zheng, M. & Storz, G. Activation of the OxyR Transcription Factor by Reversible Disulfide Bond Formation. *Science (80-.).* **279**, 11–14 (1998).
43. Greenberg, J. T., Monach, P., Chou, J. H., Josephy, P. D. & Demple, B. Positive control of a global antioxidant defense regulon activated by superoxide-generating agents in Escherichia coli. *Proc. Natl. Acad. Sci. U. S. A.* **87**, 6181–6185 (1990).
44. Faulkner, M. J. & Helmann, J. D. Peroxide Stress Elicits Adaptive Changes in Bacterial Metal Ion Homeostasis. *Antioxid. Redox Signal.* **15**, 175–189 (2011).
45. Boles, B. R. & Singh, P. K. Endogenous oxidative stress produces diversity and adaptability in biofilm communities. *Proc. Natl. Acad. Sci.* **105**, 12503–12508 (2008).
46. Gorrini, C., Harris, I. S. & Mak, T. W. Modulation of oxidative stress as an anticancer strategy. *Nat. Rev. Drug Discov.* **12**, 931–947 (2013).
47. Loewen, P. C., Switala, J. & Triggs-Raine, B. L. Catalases HPI and HPII in Escherichia coli are induced independently. *Arch. Biochem. Biophys.* **243**, 144–149 (1985).
48. Quiblier, C., Zinkernagel, A. S., Schuepbach, R. A., Berger-Bächi, B. & Senn, M. M. Contribution of SecDF to Staphylococcus aureus resistance and expression of virulence factors. *BMC Microbiol.* **11**, (2011).
49. Gutierrez, A. *et al.* β-lactam antibiotics promote bacterial mutagenesis via an RpoS-mediated reduction in replication fidelity. *Nat. Commun.* **4**, 1610 (2013).
50. Knudsen, G. M. *et al.* A third mode of surface-associated growth: Immobilization of Salmonella enterica serovar Typhimurium modulates the RpoS-directed transcriptional programme. *Environ. Microbiol.* **14**, 1855–1875 (2012).
51. Nassif, N. *et al.* A sol–gel matrix to preserve the viability of encapsulated bacteria. *J. Mater. Chem.* **13**, 203–208 (2003).
52. Dove, S. L., Smith, S. G. J. & Dorman, C. J. Control of Escherichia coli type 1 fimbrial gene expression in stationary phase: A negative role for RpoS. *Mol. Gen. Genet.* **254**, 13–20 (1997).
53. Schembri, M. A. & Klemm, P. Coordinate gene regulation by fimbriae-induced signal transduction. *EMBO J.* **20**, 3074–3081 (2001).
54. Ferenci, T. The spread of a beneficial mutation in experimental bacterial populations: The influence of the environment and genotype on the fixation of rpoS mutations. *Heredity (Edinb).* **100**, 446–452 (2008).

55. Finkel, S. E. Long-term survival during stationary phase: evolution and the GASP phenotype. *Nat. Rev. Microbiol.* **4**, 113–120 (2006).
56. Bergkessel, M., Basta, D. W. & Newman, D. K. The physiology of growth arrest: uniting molecular and environmental microbiology. *Nat. Rev. Microbiol.* **14**, 549–562 (2016).

Table 1: Catalase activity in IU

	Early Exponential Phase		Late Exponential Phase		Stationary Phase	
	HPI	HPII	HPI	HPII	HPI	HPII
wt	0.9±0.2	0.3±0.1	7.6±0.2	3.6±0.3	10.3±0.6	1.2±0.1
wt - SiO_2	6.6±0.3 (*)	0.3±0.1	6.9±0.2	1.2±0.2 (**)	10.1±0.4	1.3±0.1
ΔrpoS	1.2±0.2	0.2±0.1	10.8±0.3	0.8±0.2	10.0±0.4	1.6±0.2
ΔrpoS - SiO_2	7.6±0.3 (*)	0.2±0.1	8.2±0.2 (**)	0.6±0.2	10.8±0.5	1.3±0.1

The statistical analysis is performed comparing the following pairs of samples: the wild type with and without the addition of silica nanoparticles (*wt*-SiO_2 and *wt*), and the mutant lacking rpoS with and without the addition of silica nanoparticles (*ΔrpoS* -SiO_2 and *ΔrpoS*), at each phase of the growing curve (Early exponential, Late exponential and Stationary phases), and for the both types of catalase activity, *i. e.* hydroperoxidase I (HPI) or II (HPII). When the analysis of variance indicates differences between means, a t-test was used to differentiate the means with 95% confidence ($p < 0.05$). (*) Indicates a significant increase in catalase activity when SiO_2 nanoparticles are present in culture media; (**) Indicates a significant decrease in catalase activity when SiO_2 nanoparticles are present in culture media.

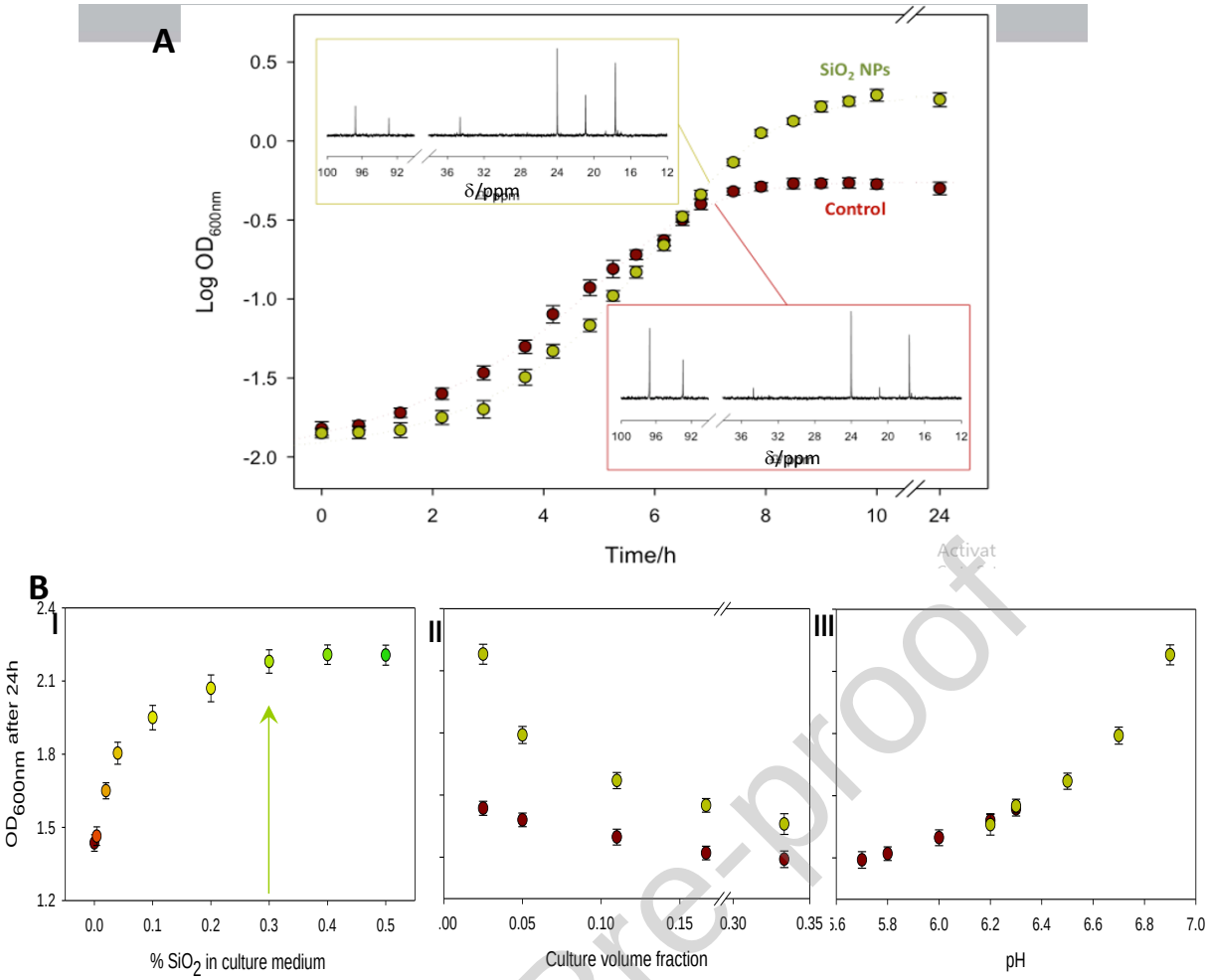

Figure 1: A- *E. coli* growing curves in minimal medium with glucose (MMG) under low aeration conditions for control sample ("Control"; brown) and for a culture supplemented with silica nanoparticle suspension (Ludox HS-40 1% w/v: "SiO_2 NPs", green). **Insets**: ^{13}C-NMR analysis of each culture media after 7 h. For the control sample, this time corresponds to the onset of the stationary phase, while the culture added with SiO_2 NPs is still in late exponential phase. Relevant chemical shifts: ethanol (δ = 17.8 ppm), lactate (δ = 21.0 ppm), acetate (δ = 24.2 ppm), succinate (δ = 35.0 ppm), glucose ($\delta_{C\alpha}$ = 93.1 ppm.; $\delta_{C\beta}$ = 96.9 ppm).
B- Effect of silica nanoparticles on cellular growth. **I**- Optical densities at 600 nm (OD_{600}) after 24h culture in MMG under high aeration as a function of silica concentration in the culture medium. The arrow indicates the condition selected for further experiments. **II**- OD_{600} after 24h as a function of culture volume fraction (denoting different aeration level conditions) for control samples (brown) and for cultures added with SiO_2 0.3% (green). **III**- OD_{600} after 24 h as a function of pH value of the culture medium for both series of samples (control: brown; SiO_2 0.3%: green).

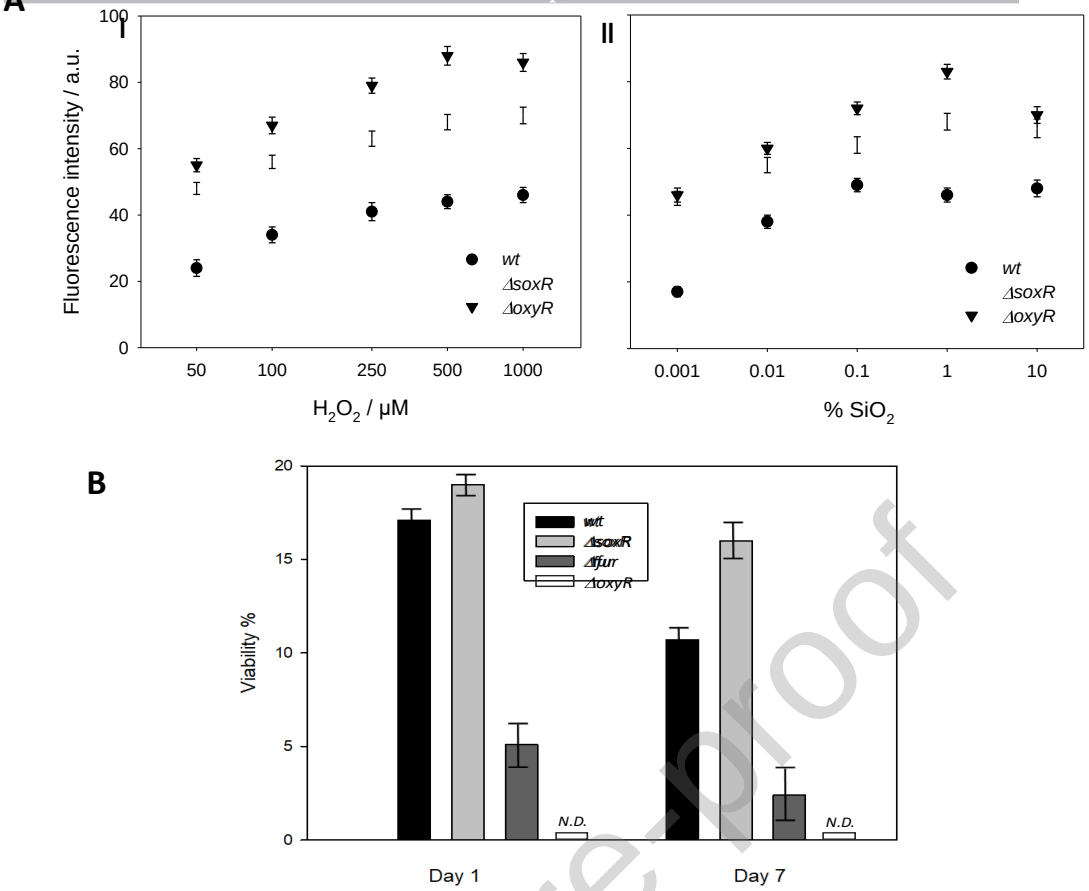

Figure 2: A- Fluorescence intensity in arbitrary units, indicative of the level of intracellular ROS generated as a function of H_2O_2 addition (**I**) and as a function of SiO_2 nanoparticles concentration in the culture medium (**II**) in samples of *E. coli wild-type*, *ΔsoxR* or *ΔoxyR*, evaluated after 30 minutes of addition. The last point corresponds to the encapsulation in a silica hydrogel (Silicate-Ludox, total silica concentration = 10%), 30 minutes after silica matrix gelation.
B- Viability (expressed as % with respect to the initial viable cells encapsulated in silicate-Ludox hydrogels) of *E. coli wild type* and mutants lacking genes involved in the redox response (*ΔsoxR, Δfur* and *ΔoxyR*). The *ΔoxyR* strain presented non detectable viability (N.D.).

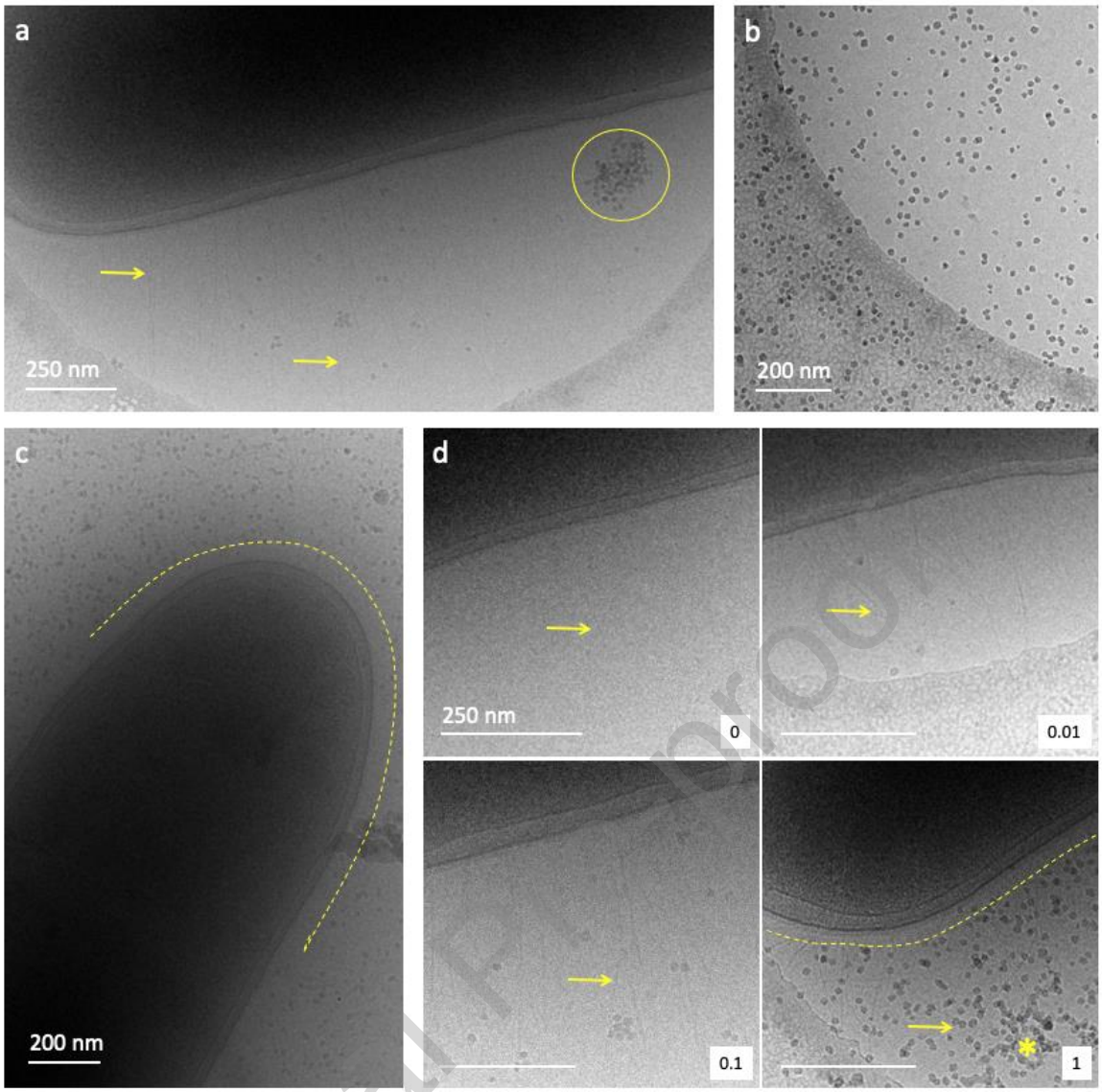

Figure 3: CryoTEM observations of bacteria/silica colloidal particles at different concentrations wt% (**a**) Aggregates of nanoparticles (yellow circle) with 0.1% and bacterial fimbriae are observed but do not interact; **(b)** homogeneous dispersion of particles at 1% that still **(c)** appear to not interact with the bacterium's wall (dotted yellow curved line) also seen in (d, 1). **(d)** Higher magnification of bacteria walls with no silica, 0.01, 0.1 and 1% of silica colloidal particles wt%. The presence of fimbriae (yellow arrows) appears to increase with the silica concentration. * indicates possibly the presence of frozen ethane from the preparation.

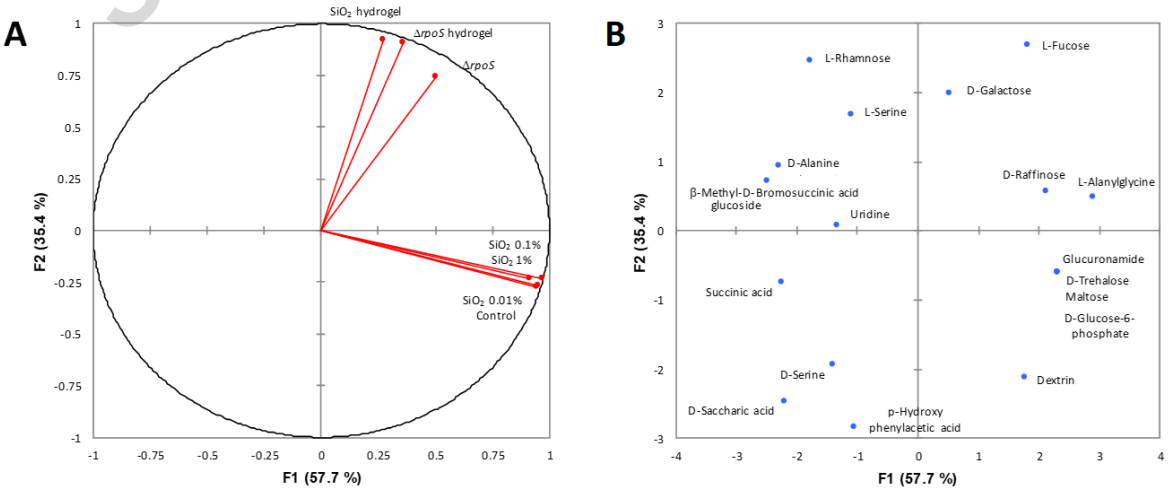

Figure 4: Principal component analysis (PCA) was performed on a subset of carbon sources (C-sources) were changes in the degree of utilization were evidenced in at least one treatment. Two main components explaining the 93.1% of the total variation, F1 (57.7 %) and F2 (35.4 %), were selected,

and both the variables (different treatments) and the observations (C-sources) were projected on these two axes of the PCA.

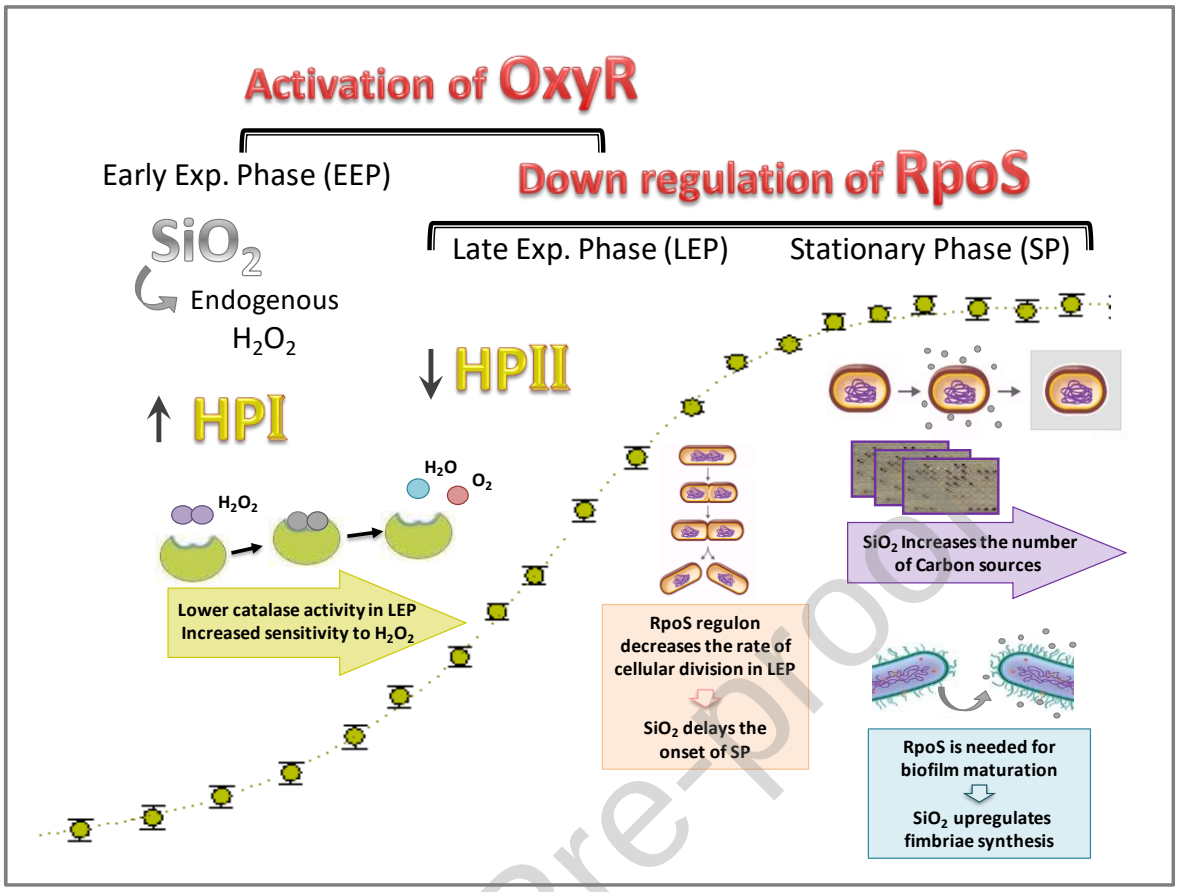

Figure 5: Schematic representation of the effect of the addition of SiO_2 nanoparticles or the encapsulation in silica on *Escherichia coli* K-12, summarising the observed experimental results presented in Table I and in Figures 1 to 4.

Declaration of interests

☐ The authors declare that they have no known competing financial interests or personal relationships that could have appeared to influence the work reported in this paper.

☒ The authors declare the following financial interests/personal relationships which may be considered as potential competing interests:

Mercedes Perullini reports financial support was provided by EULASUR.

Highlights

- We focus on the specific biologic responses caused by silica on *Escherichia coli.*
- Silica promotes the induction of alternative metabolic pathways and the increase of growth.
- The alterations in growing cultures are not triggered by the initial oxidative ROS response.
- Our results suggest the induction of *rpoS* polymorphism.
- Cell physiological adaptation to silica opens perspectives in the design of bioactive devices.